Wind driven Induction Generator with Vienna Rectifier and PV for Hybrid Isolated Generations

S. Singaravelu, G. Balasubramanian

Abstract— Hybrid PV-wind generation shows higher availability as compared to PV or wind alone. For rural electrifications, researches are focused on hybrid power system which provides sustainable power. The variable voltage and frequency of the self excited induction generator (SEIG) is rectified through Vienna rectifier (three switches) to the required D.C voltage level and fed to common D.C bus. The variable output voltage of PV module is controlled by DC/DC converter using proposed fuzzy logic controller and fed to common D.C bus. The DC bus collects the total power from the wind and photovoltaic system and used to charge the battery as well as to supply the A.C loads through inverter. A dynamic mathematical model and MATLAB simulations for the entire scheme is presented. Results from the simulations and experimental tests bring out the suitability of the proposed hybrid scheme in remote areas.

Index Terms — DC-DC converter, Fuzzy logic, SEIG, PV array, Vienna Rectifier, and Wind energy.

I. INTRODUCTION

Hybrid distributed generators are gaining prominence over the conventional energy conversion due to great advantages like being abundant in nature, recyclable and causing too less pollution [1-3]. There are number of schemes based on wind and PV resources. One such a scheme is a self excited wind driven induction generators is proposed for isolated applications and they are found to be integrated easily to the utility network is required [4]. An intelligent controller for a stand-alone hybrid generation system was discussed by [2]. It comprises the wind and solar systems integrated to a common DC bus through the necessary power electronic interface. The power electronic interface consists of a conventional rectifier which consists of six switches. In this paper a Vienna rectifier [5] have been used which can generate three voltage level with decreased number of power switches (only three), thus simplifying the control and reducing cost. It also leads to reduced blocking voltage stress on power semi conductors which can enhance reliability.

The capacitor bank connected across the SEIG is selected such that it can meet the reactive power requirement under full load and wide speed range. In addition the photovoltaic array can supply the additional reactive power requirement (through proposed fuzzy logic MPPT controller) to the load to some extent.

Figure 1 describes the hybrid scheme of solar-wind with the proposed fuzzy logic controller. A self-excited induction generator (SEIG) connected in parallel with the inverter through Vienna rectifier. Vienna rectifier will convert the A/C supply into common D/C supply with reduced (desired) output voltage thus in turn reduces the combined work of ordinary rectifier and D/C–D/C buck converter [2].

Dr.S.Singaravelu, Electrical Engineering, Annamalai University, Annamalainagar, India.
G.Balasubramaniaan, Electrical Engineering, Annamalai University, Annamalainagar, India.

The variable output voltage of PV module is controlled by DC/DC converter using proposed fuzzy logic MPPT controller and fed to common D.C bus. The DC bus then collects the total power from the wind and photovoltaic system and used to charge the battery as well as to supply the A.C loads through inverter.

The proposed configuration is compared to the conventional six-switch two level converter systems by way of simulation which shows that the Vienna rectifier topology
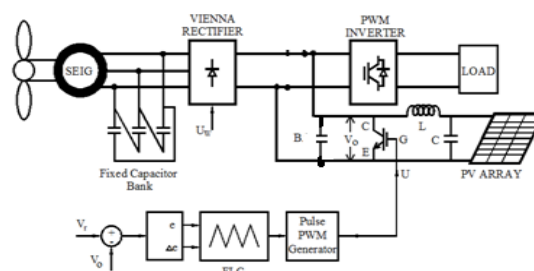

Figure 1. Schematic diagram of solar-wind hybrid scheme

has better efficiency and the potential for better reliability.

The complete system is modeled and simulated MATLAB/ Simulink environment. The inverter output is controlled through PWM generator such that desired output voltage and frequency can be achieved. The THD spectrum obtained using simulation for both conventional six pulse converter and Vienna rectifier are also presented. Results from simulations and experimental shows the dynamic reactive power compensation is inherent.

II. PV ARRAY MODELING

Figure 2 shows the equivalent circuit of a PV cell. A PV cell can be represented by an equivalent circuit [6] as shown in Figure 2. The characteristics of this PV cell can be obtained using standard equation (1).

$$I = I_{PV} - I_O \left[\exp\left(\frac{V + R_S I}{V_t a} \right) - 1 \right] - \frac{V + R_S I}{R_p} \tag{1}$$

I_{PV} = photovoltaic current

I_O = saturation current

V_t = N_S k T/q, thermal voltage of array

Ns = cell connected in series

T = is the temperature of the p-n junction

k = Boltzmann constant

q = electron charge

R_S = equivalent series resistance of the array

R_P = equivalent parallel resistance of the array

a = diode ideality constant

Figure 2 shows the single diode model. A single solar cell will produce only a limited power. Therefore it is usual practice in order to get desired power rating the solar cells are

connected in parallel and series circuits which form a module. Such modules are again connected in parallel and series to form a solar array or panel to get required voltage and current. The equivalent series and parallel resistance of the array are denoted by the symbol R_S and R_P respectively in the equivalent circuit.
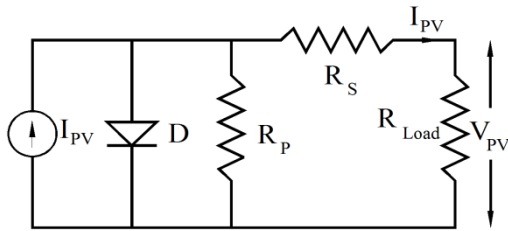

Figure 2: Equivalent circuit of PV cell

From the general *I-V* characteristic of the practical photovoltaic device one can observe that the series resistance R_S value will dominate in the voltage source region and the parallel resistance R_P value will dominate in the current source region of operation.

The general equation of a PV cell describes the relationship between current and voltage of the cell. Since the value of shunt resistance R_P is high compared to value of series resistance R_S the current through the parallel resistance can be neglected. The light generated current of the photovoltaic cell depends linearly on the solar irradiation and is also influenced by the temperature [7] given by the equation (2)

$$I_{PV} = \left[I_{PV,n} + K_I \, \Delta_T \right] \frac{G}{G_n} \tag{2}$$

$I_{PV,n} =$ is the light generated current at nominal condition (25^0C and 1000 W/ m^2)

Δ_T = $T - T_n$

T = actual temperature [K]

T_n = nominal temperature [K]

K_I = current coefficients

G = irradiation on the device surface [W/m^2]

G_n = nominal irradiation

$$I_O = \frac{I_{sc,n} + K_I \Delta_T}{exp\left(\frac{V_{oc,n} + K_V \Delta_T}{aV_t}\right) - 1} \tag{3}$$

K_V = voltage coefficients

K_I = current coefficients

The current and voltage coefficients K_V and K_I are included as shown in equation (3) in order to take the saturation current I_O which is strongly dependent on the temperature.

The output voltage is increased (where the current remain unchanged) proportionally on number of identical PV modules connected in series (N_{ser}). Similarly the output current is increased (where the voltage remain unchanged) proportionally on number of identical PV modules connected in parallel (N_{par}). It can be noted that the equivalent series and parallel resistance are directly proportional to the number of series modules and inversely proportional to the number of parallel modules respectively. The equation for array composed of N_{ser} x N_{par} given by equation (4)

$$I = I_{PV}N_{par} - I_O N_{par}\left[\exp\left(\frac{V + R_S\left(\frac{N_{ser}}{N_{par}}\right)I}{V_t a N_{ser}}\right) - 1\right] - \frac{V + R_S\left(\frac{N_{ser}}{N_{par}}\right)I}{R_P\left(\frac{N_{ser}}{N_{par}}\right)} \tag{4}$$

I_{mp}	4.40 A	V_{oc}	21.20 V
V_{mp}	17.00 V	a	1.3
P_{max}	74.8 W	R_{se}	0.511 Ω
I_{sc}	5.02 A	R_{sh}	44.25 Ω
N_s	36	K_v	-74.7 mv/°C
$I_{O,n}$	9.83 x 10^{-8}A	K_I	2.80 mA/°C

Table I. Parameter of KCP -12075 solar array at 25°C, 1000W/m^2

The parameter of solar array (KCP -12075 at 25℃, 1000W/m^2) used for theoretical and experimental setup is given in table I.

III. DYNAMIC MODELING OF SEIG

The d-q representation of induction generator is shown in Figure 3. The dynamic equations [8] governing the stator and the rotor currents in the stator flux coordinates can be written as follows

$$L_s \frac{d}{dt}(i_{sq}) = v_{sq} - R_s i_{sq} - (\omega_{ms})(L_s i_{sd} + L_o i_{rd}) - L_o \frac{d}{dt}(i_{rq}) \tag{5}$$

$$L_s \frac{d}{dt}(i_{sd}) = v_{sd} - R_s i_{sd} + (\omega_{ms})(L_s i_{sq} + L_o i_{rq}) - L_o \frac{d}{dt}(i_{rd}) \tag{6}$$

$$L_r \frac{d}{dt}(i_{rq}) = v_{rq} - R_r i_{rq} + (\omega_{ms} - \omega_e)(L_r i_{rd} + L_o i_{sd} - L_o d dt i_{sq}) \tag{7}$$

$$L_r \frac{d}{dt}(i_{rd}) = v_{rd} - R_r i_{rd} + (\omega_{ms} - \omega_e)(L_r i_{rq} + L_o i_{sq} - L_o d dt i_{sd}) \tag{8}$$

The modeling of the excitation system are given below

$$\frac{d}{dt}(v_{sd}) = 1/C(i_{sd} - i_{Ld} + i_d) + \omega_{ms} v_{sq} \tag{9}$$

$$\frac{d}{dt}(v_{sq}) = 1/C(i_{sq} - i_{Lq} + i_q) - \omega_{ms} v_{sd} \tag{10}$$

The modeling of Inverter – dc-dc converter - battery system

$$\frac{d}{dt}(i_{id}) = 1/L_f(v_{id} - R_f - v_{sd}) + \omega_{ms} i_{iq} \tag{11}$$

$$\frac{d}{dt}(i_{iq}) = 1/L_f(v_{iq} - R_f - v_{sq}) - \omega_{ms} i_{id} \tag{12}$$

The modeling of resistive load

$$\frac{v_{sd}}{R_L} = i_{Ld} \text{ And } \frac{v_{sq}}{R_L} = i_{Lq} \tag{13}$$

where,

$$\Psi_{sq} = -L_{ls}i_{sq} - L_m(i_{rq} + i_{sq}), \; \Psi_{sd} = -L_{ls}i_{sd} - L_m(i_{rd} + i_{sd})$$

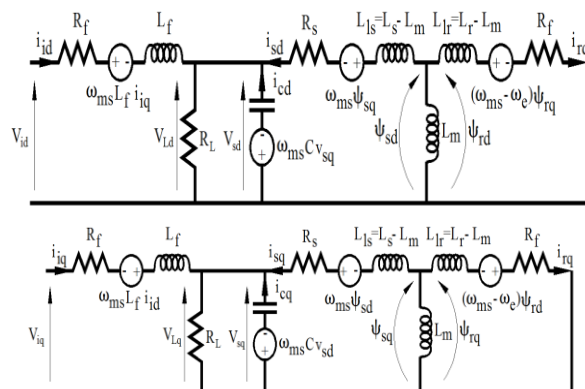$$\Psi_{rd} = -L_{lr}i_{rd} - L_m(i_{rd} + i_{sd}) \text{ and } \Psi_{rq} = -L_{lr}i_{rq} - L_m(i_{rq} + i_{sq})$$

Figure 3. d-axis and q-axis equivalent circuit

IV. DC-DC BOOST CONVERTER

A dual stage power electronic system comprising a boost type dc-dc converter and an inverter is used to feed the power generated by the PV array to the load. To maintain the load voltage constant a DC-DC step up converter is introduced between the PV array and the inverter. The block schematic of the proposed scheme is shown in Figure 1. In this scheme a PV array feeds DC-DC converter used in step-up configuration. The voltage across the DC-DC converter is fed to a three-phase, PWM inverter a three -phase fixed amplitude and fixed frequency supply is obtained to feed an isolated load. For a dc-dc boost converter, by using the averaging concept, the input–output voltage relationship for continuous conduction mode is given by

$$Vo/Vin = 1/(1 - D) \qquad (14)$$

Where, D = duty cycle. Since the duty ratio "D" is between 0 and 1 the output voltage must be higher than the input voltage in magnitude.

It should be noted that the control logic of such dc-dc converter has to be different when it is fed from a stiff DC source. The duty ratio of the chopper is found to increase linearly with increase in cell temperature and hence the intensity. As the inverter DC voltage varies with irradiation to obtain constant amplitude and constant frequency supply from the inverter, a closed loop fuzzy controller is incorporated to automatically vary the duty-cycle of the DC-DC converter to obtain constant DC voltage at the inverter input terminals. The inverter output is then applied to an isolated load. At the same time fuzzy controller will maintain the output voltage of inverter by supplying the required reactive power according to the change in speed of the wind and load. This can be achieved by maintaining the battery voltage adequately high.

V. FUZZY LOGIC MPPT CONTROLLERS

The conventional PI controllers are fixed-gain feedback controllers. Therefore they cannot compensate the parameter variations in the process and cannot adapt changes in the environment. PI-controlled system is less responsive to real and relatively fast alterations in state and so the system will be slower to reach the set point. On the other hand P&O method for MPPT tracking will not respond quickly to rapid changes in temperature or irradiance. Therefore the fuzzy control algorithm is capable of improving the tracking performance as compared with the classical methods for both linear and nonlinear loads. Also, fuzzy logic is appropriate for nonlinear control because it does not use complex mathematical equation.

The two FLC input variables are the error E and change of error ΔE. The behavior of a FLC depends on the shape of membership functions of the rule base. In this paper a fuzzy logic control scheme (Figure 1) is proposed for maximum solar power tracking of the PV array with an inverter for supplying isolated loads. They have advantages to be robust and relatively simple to design since they do not require the knowledge of the exact model. On the other hand the designer needs complete knowledge of the hybrid system operation.

A. Fuzzification

The membership function values are assigned to the linguistic variables using seven fuzzy subset called negative big (nb), negative medium (nm), negative small (ns), zero(zr), positive small (ps), positive medium (pm), positive big (pb). Fuzzy associative memory for the proposed system is given in Table-2. Variable e and Δe are selected as the input variables, where e is the error between the reference voltage ($V_{er.}$) and actual voltage (V_o) of the system, Δe is the change in error in the sampling interval. The output variable U is the reference signal for PWM generator. Triangular membership functions are selected for all these process. The range of each membership function is decided by the previous knowledge of the proposed scheme parameters.
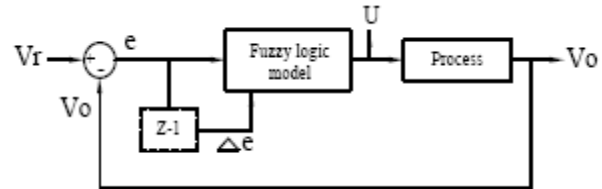

Figure 4. Fuzzy Logic Control Scheme

B. Inference engine

Inference engine mainly consist of Fuzzy rule base and fuzzy implication sub blocks. The inputs are now fuzzified are fed to the inference engine and the rule base is then applied. The output fuzzy set are then identified using fuzzy implication method. Here we are using MIN-MAX fuzzy implication method.

C. Defuzzification

Once fuzzification is over, output fuzzy range is located. Since at this stage a non-fuzzy value of control is available a defuzzification stage is needed. Centroid defuzzification method [9] is used for defuzzification in the proposed scheme. The membership function of the variables error, change in error and change in reference signal for PWM generator are given in Table 2.

Table 2. Fuzzy associative memory for the proposed system

e	Δe						
	nb	nm	ns	zr	ps	pm	pb
nb	nb	nb	nb	nm	nm	ns	zr
nm	nb	nb	nm	nm	ns	zr	ps
ns	nb	nm	nm	ns	zr	ps	pm
zr	nm	nm	ns	zr	ps	pm	pm
ps	nm	ns	zr	ps	pm	pm	pb
pm	ns	zr	ps	pm	pm	pb	pb
pb	zr	ps	pm	pm	pb	pb	pb

VI. VIENNA RECTIFIER

The use of Vienna rectifier is visualized instead of a conventional six pulse converter. Vienna rectifier is three pulses A/C –D/C converter .The switching losses are minimized in this rectifier to 50% as that of a conventional six pulse one. By properly controlling the PWM pulses applied to three switches the D/C bus voltage across the two split capacitor C1and C2 is maintained at a constant value.

At the same time the THD of the input current is reduced drastically compared to the normal six switch converter. The power circuit of Vienna Rectifier is shown in Figure 5. Where, D1 to D6 are fast recovery diode, D_{Ai}, D_{Bi}, D_{Ci}, i = 1to4 are slow recovery diode, S_A, S_B, S_C are power switches with freewheeling diodes, C_1, C_2 are equal capacitance connected across the output of the rectifier and its centre point of C_1, C_2 is connected to all the three switches. When rectifier is acting as positive boost converter C_1 is charged

more. When rectifier is acting as negative boost converter C_2 is charged more .When no switches are 'ON' both C_1 and C_2 are charged equally. By properly controlling the PWM pulses applied to three switches the D/C bus voltage across the two split capacitor C_1 and C_2 are maintained at constant values.
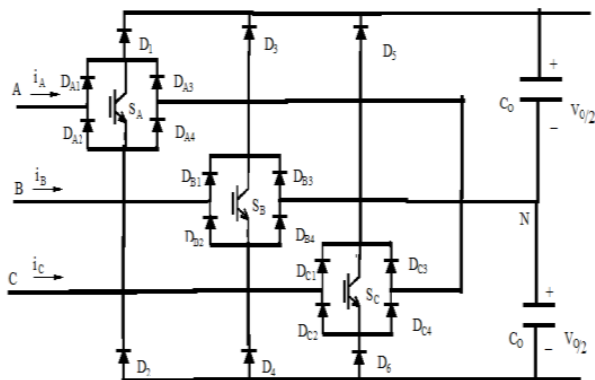

Figure 5. Vienna Rectifier circuit

The theory of self excitation is used for induction generators using capacitor banks connected at the terminals of the machine. The energy to charge the capacitor banks is not from the D/C bus because the Vienna rectifier is unidirectional in nature.

The simplified Fourier expression of a periodic non sinusoidal waveform is expressed as:

$$V(t) = V_{o+}V_1 sin(\omega t) + V_2 sin(2\omega t) + V_3 sin(3\omega t) + \cdots + V_n sin(n\omega t) \qquad (15)$$

$$V(t) = V_{o+} \Sigma(a_k cos(\omega t) + b_k sin(\omega t)) \quad (16)$$

for k= 1 to α

Where a_k and b_k are the coefficient of the individual harmonic terms components.

Under certain conditions, the cosine or sine terms may vanish to yield a simpler expression. If the function is an even function, meaning f (-t) = f (t), then the sine terms vanish from the expression. However if the function is odd, with f (-t) = -f (t), then the cosine term disappear. It is to be noted that having both sine and cosine terms affects only the displacement angle of the harmonic components and the shape of the nonlinear wave and does not alter the principle behind the application of the Fourier series.

The coefficient of the harmonic terms of a function f (t) contained in Equation (16) are determined by:

$$a_k = \frac{1}{\pi} \int_{-\pi}^{+\pi} f(t).\cos kt. dt, \ (k = 1,2,3 \dots. n) \qquad (17)$$

$$b_k = \frac{1}{\pi} \int_{-\pi}^{+\pi} f(t).\sin kt. dt, \ (k = 1,2,3 \dots. n) \qquad (18)$$

The coefficients represent the peak values of the individual harmonics frequency terms of the nonlinear periodic function represented by f (t). The input current that flows through the switch is governed by

$$i_a(t) = \frac{v_i \sqrt{2}}{2 \pi f L \sqrt{3}} (1 - cos\omega t) \qquad (19)$$

The phase currents during this time follow

$$\frac{d}{dt} i_a(t - t_o) = \frac{v_a (t - t_o)}{L} - \frac{v_o}{3L} \qquad (20)$$

The solution of equation (20) yields a set of equations

$$i_a(t) = \frac{\sqrt{2}v_i}{3\omega L}(\sqrt{2} sin\omega t + 3cos\omega t - 3) - \frac{v_o}{3L} +$$

$$3\sqrt{2}v_i + \frac{2\sqrt{3}\sqrt{2}v_i - 2\pi v_o}{6\omega L} \qquad (21)$$

Which describe the line currents as a function of the load voltage .The equivalent circuit is constructed using equations written similarly for the three phases.

VII. RESULT AND DISCUSSION

The photovoltaic *I-V* and *P-V* characteristics, the capacitance requirements of SEIG are discussed. A MATLAB based modeling and simulation scheme (Appendix) with fuzzy logic controller is proposed, which are suitable for studying dynamic characteristics of the hybrid scheme under varying speed and load conditions (Figure1). The advantage of Vienna is highlighted through THD comparisons.

A. PV-Characteristics

The behavior of the PV cells and its characteristics are discussed in this section. It is found that the set of *P-V* and
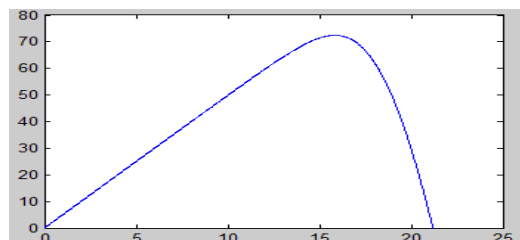

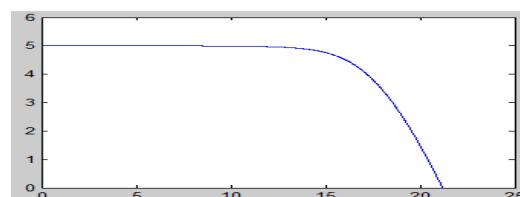Figure 6(a): P-V Characteristics

Figure 6(b): I-V Characteristics

I-V characteristics are highly nonlinear and dependent on solar irradiance of the PV array. Figure 6(a) and 6(b) shows P-V and I-V characteristics of a PV cell. It can be observed that as the cell temperature remain constant the PV output voltage remains nearly constant while the PV output current increases with increasing solar intensity.

B. Capacitance requirements of SEIG to maintain desired terminal voltage under varying load and speed

Capacitance VAR requirement to maintain the required terminal voltage under varying load and speed conditions are given in Figure 7(a) and 7(b).
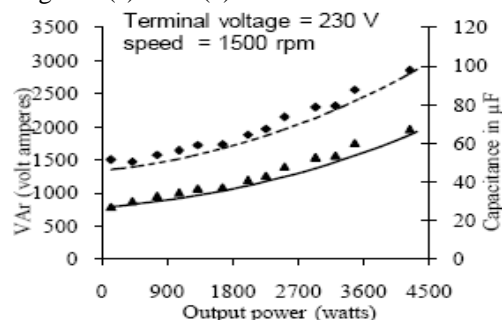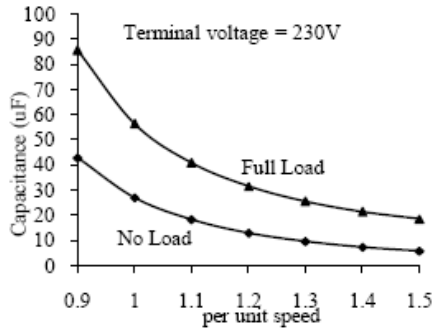

Figure 7(a)

Figure 7(b)

Figure 7 Capacitance and VAR requirements with change in load and speed

Figure 7(a) shows variation of the reactive VAR and capacitance with output power for constant terminal voltage at rated speed. For constant terminal voltage, the value of capacitance and VAR's increases with output power. It may also be seen that for an increase in output power of the machine at rated speed, the reactive VAR has to vary continuously for regulating the terminal voltage. Figure 7(b) shows the variation of speed with capacitance value to maintain constant rated terminal voltage under no load and loaded condition of the generator. It may be noted that, as the speed increases, the capacitance requirements are reduced at full load and no load. It is also observed that, the generator requires higher value of capacitance at full load when compared to no load conditions.

C. Dynamic Response of hybrid scheme

The simulated per phase current and voltage waveform across the load is shown in Figure 8(a). The simulated per phase current waveform (Fig. 8(b)) shows, even though the load is applied at 1.5 seconds the voltage across the load remains almost constant. Figure 8(c) and 8(d) shows the experimental waveforms of current and voltage respectively under loading conditions.
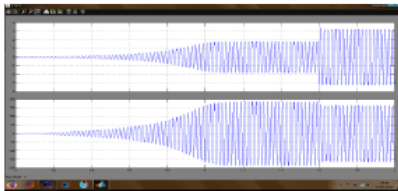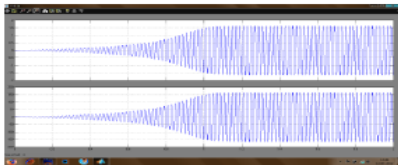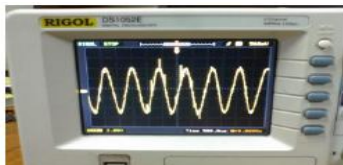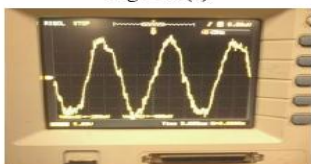

Figure 8(a)

Figure 8(b)

Figure 8(c)

Figure 8(d)

Figure 8: Simulated and Experimental waveforms

D. Harmonic analysis of Vienna Rectifier over Conventional Rectifier

The THD spectrum obtained using MATLAB simulation for both conventional six pulse converter and Vienna rectifier is shown in Figure 9(a) and 9(b). I
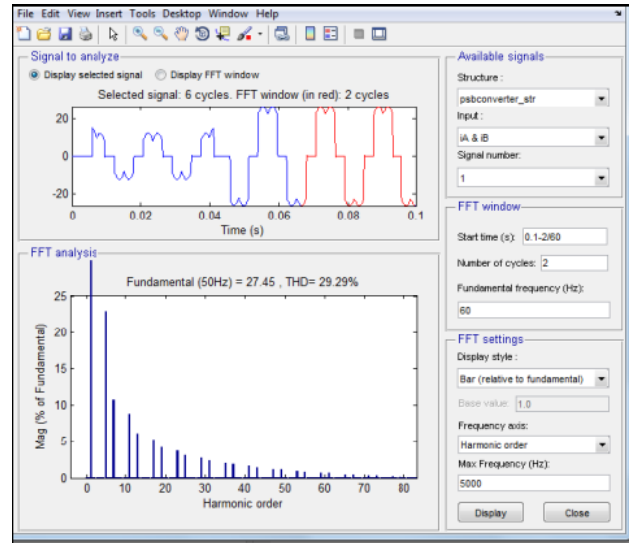

Figure 9(a) Conventional Six Pulse Converter

It is clear that the Vienna rectifier offers a low THD value of 2.59% than the six pulse converter value of 29.29%.When the load is allowed to increase, the power switch in the relevant phase is activated, enabling the capacitors to be suitably charged in order to maintain the voltage across the load. Per phase input voltage and current waveform of Vienna rectifier is shown in Figure 9(c).
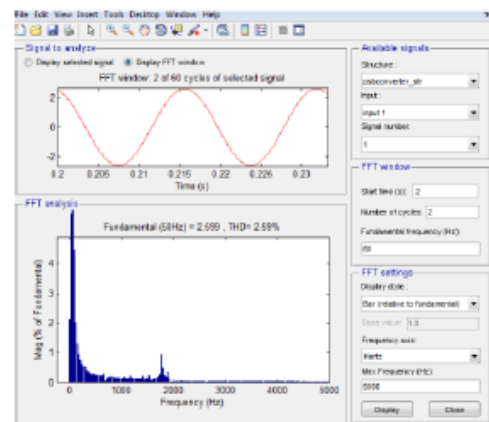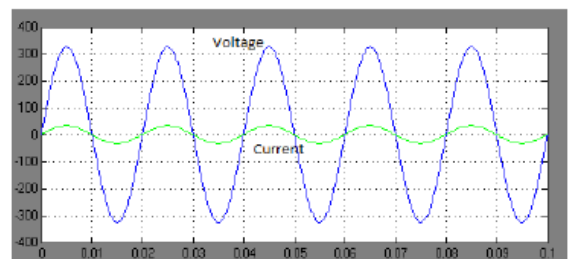

Figure 9(b) Vienna rectifier

Figure 9(c) per phase input voltage and current waveforms of Vienna rectifier

VIII. CONCLUSION

A hybrid scheme for isolated applications, employing solar and wind driven induction generator with Vienna rectifier, is proposed with fuzzy logic controller, with optimized rule-base. Hence it is very suitable for the rural electrification in remote areas where grid cannot be accessed.

The photovoltaic characteristics and capacitance requirements of SEIG are discussed. Using the mathematical model described the dynamic characteristics of the hybrid scheme to maintain almost the desired load voltage is also discussed. The simulated results are focused on both the steady-state and dynamic behavior of the hybrid scheme which demonstrates the validity of the proposed model. The simulation and the experimental result of hybrid scheme shows the operation of the controller for constant load voltage had inherently resulted in balancing of power between the two sources while supplying constant power to the load.

IX. APPENDIX

A MATLAB based modeling and simulation scheme along with fuzzy controller for both Vienna rectifier and D.C/D.C converter is proposed (Figure.10) which are suitable for analysis of complete hybrid scheme.
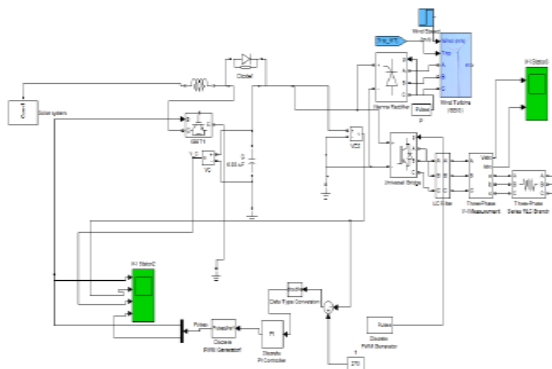

Figure 10 Hybrid scheme solar/wind with Vienna Rectifier

The proto type model of the Vienna Rectifier shown in Figure 12 built for 230V, 2A, 1Kw. PV array in the proposed scheme consists of solar PV array of 74.8W, 21.2V, 4.4A. A load of 80Ω per-phase was connected in star across the inverter terminals. A DC-DC converter (L=40μH, C=0.025F) was constructed with IGBT (40 A, 600 V) as a switch with a switching frequency of 2 KHz shown in Fig.13. The closed loop firing scheme was employed to trigger the DC-DC converter. A 50Hz, three-phase IGBT inverter was fabricated, and a microcontroller PIC 16F877A was used to trigger the IGBT in 180 degree conduction mode.

Figure 11: Self-Excited Induction generator (driven by D.C motor for variable speed)

Figure 12 Vienna rectifier

The above scheme was tested for different speed and load. Similar PIC 16F877A was used to trigger the IGBT switches of Vienna Rectifier.

EXPERIMENTAL SETUP AND MACHINE PARAMETERS

Details of Experimental setup of SEIG (Figure 11)

Specifications of the Induction Generator, three-phase, 50Hz, four-pole, 230V, 2A, 0.75 kW

Figure 13 DC-DC-Converters - Inverter

Machine parameters in per-phase

Stator resistance $R_S = 9.1\Omega$
Rotor resistance $R_r = 11.8\Omega$
Stator and rotor leakage reactance $X_{ls} = X_{lr} = 11.9\Omega$

Magnetization curve – linearized as

$V_g/a = 260.68 - 0.523X_M, \quad X_M \leq 140\Omega$
$V_g/a = 410.81 - 1.5415X_M, \quad X_M > 140\ \Omega$

X. ACKNOWLEDGMENT

The authors gratefully acknowledge the support and facilities provided by the authorities of Annamalai University, Annamalainagar, Tamilnadu, India to carry out this research work.

REFERENCES

[1] Y.Jaganmohan Reddy, Y.V. Pavan kumar, K. padma raju, and Anil kumar ramesh, " Retrofitted Hybrid Power System Design With Renewable Energy Sources for Buildings", IEEE Transaction on Smart Grid , Vol.3, no.4, pp. 2174-2186, Dec 2012.

[2] S.Meenakshi, K.Rajambal, C.Chellamuthu, and S.Elangovan, "Intelligent Controller for Stand-Alone Hybrid Generation System", *Power India Conference IEEE*, pp 8-15, 2006.

[3] Ashraf A.Ahmed, Li Ran, Jim Bumby, "Simulation and control of a Hybrid PV-Wind System", *Power Electronics Machines & Drives, PEMD 4th IET conference*, pp 421-425, 2008.

[4] Meenakshmisundaram Arutchelvi, Samuel Arul Daniel, "Grid Connected Hybrid Dispersed Power Generators Based on PV Array And Wind Driven Induction Generator", Journal of Electrical Engineering, Vol., 60, pp 313-320, 2009.

[5] Hao Chen, Dionysios C. Aliprantis , " Analysis of Squirrel-cage Induction Generators with Vienna Rectifier for Wind Energy Conversion System", IEEE Transactions on Energy Conversion, Vol.26, no.3, 2011.

[6] M.G.Villalva, J.R.Gazol, and E.R.Filho, "Comprehensive Approach to Modeling and Simulation of Photovoltaic Arrays", *IEEE trans. on Power Electronics*, vol.24, no.5, pp.1198-1208, 2009.

[7] H. Patel, and V. Agarwal, "MATLAB based modeling to study the effects of partial shading on PV array characteristics", *IEEE trans. on energy conv*., vol. 23, no.1, pp. 302-310, 2008.

[8] A.Karthikeyan, C.Nagamani, G.Saravana Illango, A.Sreenivasulu, "Hybrid, open-loop excitation system for a wind turbine –driven stand-alone induction generator", *IET Renewable Power Generation,* Vol.5, no.2,pp.184-193,2011.

[9] Timothy and Ross J, Fuzzy logic with engineering applications, McGraw hill international editions, Electrical engineering series, New York, 1997.